

Relationship Between the Ligand Structure and the Luminescent Properties of Water-Soluble Lanthanide Complexes Containing Bis(bipyridine) Anionic Arms

Loïc J. Charbonnière,*^[a] Nicolas Weibel,^[a] Pascal Retailleau,^[b] and Raymond Ziessel*^[a]

Abstract: A series of six new ligands (**L**¹–**L**⁶) suitable for the formation of luminescent lanthanide complexes in water is described. Ligands **L**¹–**L**⁴ are constructed from two 6'-carboxy-6-methylene-2,2'-bipyridine chromophoric arms bonded to the amino function of a 2-aminomethylene-6-carboxy-pyridine (**L**¹), an *N,N*-diacetate-ethylene diamine (**L**²), a serine (**L**³), or an aminomalonic acid (**L**⁴). For ligands **L**⁵ and **L**⁶, the linking amino function is provided by a glutamic acid, and the anionic functions at the 6'-position of the bipyridyl arms are made of the sodium salts of monoethylphosphonic

ester (**L**⁵) and phosphonic acid (**L**⁶). The synthesis and characterisation of the ligands are described, together with the study of the formation of lanthanide complexes with europium and terbium. In the case of **L**³, the europium complex obtained in acidic conditions was crystallised and the X-ray crystal structure is depicted. Photophysical properties of the complexes were studied by means of UV-visible

absorption, and steady-state and time-resolved luminescence spectroscopy. Excited-state luminescence lifetimes of the complexes were determined in water and deuterated water to gain insight into the number of water molecules directly coordinated in the first coordination sphere of the complexes. The coordination behaviour of the series of ligands is questioned in the light of the spectroscopic data and discussed in terms of protection of the cation towards water molecules and their impact on the luminescence efficiency.

Keywords: europium • lanthanides • ligand design • luminescence • terbium

Introduction

Lanthanide complexes are becoming ever more important in the field of analytical biochemistry, in which they are used in prominent applications in nuclear magnetic reso-

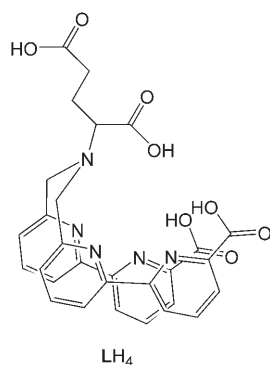
nance imaging,^[1] as magnetic probes for structural determination of proteins^[2] and biological environments.^[3] The development of lanthanide-based probes for luminescence applications has attracted much interest owing to their exceptional photophysical properties.^[4,5] The strongly forbidden character of f–f electronic transitions has resulted in very long luminescence excited-state lifetimes, which in some cases can reach the millisecond range for europium or terbium complexes. However, this property results in a major photophysical drawback in these compounds. Molar absorption coefficients of the f–f transitions of lanthanides rarely exceed unity and their direct excitation appears difficult necessitating laser excitation. This inconvenience has nevertheless been bypassed by the introduction of the so-called antenna effect,^[6] which consists of embedding the lanthanide cations into an organic framework containing chromophoric units. The role of the ligand is first to absorb light and to transfer this excess energy to the lanthanide excited states, but also to complete the first coordination sphere of the metal in order to prevent luminescence quenching due to vibrational deactivation through O–H, N–H and C–H oscillators of the solvent molecules.^[7,8] The overall luminescence

[a] Dr. L. J. Charbonnière, Dr. N. Weibel, Dr. R. Ziessel
Laboratoire de Chimie Moléculaire
UMR 7509-CNRS Ecole de Chimie, Polymères et Matériaux
25 rue Becquerel, 67087 Strasbourg Cedex 02 (France)
Fax: (+33)3-90-24-26-35
E-mail: charbonn@chimie.u-strasbg.fr
ziessel@chimie.u-strasbg.fr

[b] Dr. P. Retailleau
ICSN-CNRS, 1 avenue de la Terrasse
91198 Gif sur Yvette (France)

Supporting information for this article is available on the WWW under <http://www.chemeurj.org/> or from the authors. Full experimental description of the intermediate compounds **5**, **6**, **8**, **9**, **10**, **13**, **14**, **16**, **17**, and **20**, and their characterisation, full description of the crystal structure determination of [Eu(**L**³H₂)Cl]Cl·3H₂O, and table of the relative intensities of the ³D₀→⁷F₂/^βD₀→⁷F₁ transitions of the europium complexes (17 pages).

efficiency of a lanthanide complex (Φ_{ov}) is the product of the efficiency of the ligand to sensitise the lanthanide (η_{sens}) and the efficiency of the lanthanide to emit photons once in its excited state (Φ_{Ln}). The exact parameters governing the sensitisation process are still unclear, despite comprehensive works on the matter, which have led to general rules on the optimisation of the ligand-centred energy levels.^[9] The central question arises in the exact mechanism of sensitisation, and whether excitation is shuttled through the ligand-centred triplet excited state or if direct excitation of the lanthanide is possible by the singlet excited state of the ligand.^[10] Concerning the shielding of the metal cation by the ligand,



coordination numbers of eight to ten are commonly observed for lanthanide complexes, and nona- or decadentate ligands are particularly targeted.

In prior work in the field, we disclosed^[11] that the Eu and Tb complexes formed with the octadentate ligand **L** are very good probes for luminescence microscopy^[12] and time-resolved fluoroimmunoassays.^[13] Based on a glutamate skeleton functionalised on the amino function by two 6-carboxy-bipyridine arms, this ligand

formed complexes with the generic formula $[Ln(L)(H_2O)]$ upon coordination with lanthanide cations in water. The resulting Eu and Tb complexes are highly luminescent with long-lived luminescence lifetimes (τ) despite the presence of a single water molecule in the first coordination sphere of the cations. The removal of this water molecule would undoubtedly be beneficial to the photophysical parameters such as Φ_{ov} , Φ_{Ln} , and τ . Up to now, all our efforts to crystallise such complexes failed. Gaining insight into the molecular structure would allow for the localisation of the water molecule, for a better understanding of its interactions with the surroundings and would provide new ideas for removal of the water molecule. It is surmised that the utilisation of an additional chelating donor atom is an attractive approach to increase the coordination number, providing that it is well placed in the ligand architecture.

Figure 1 summarises the different coordination modes envisaged for $[Ln(L)(H_2O)]$ assuming that the ligand is coordi-

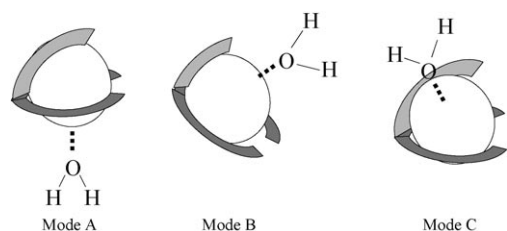
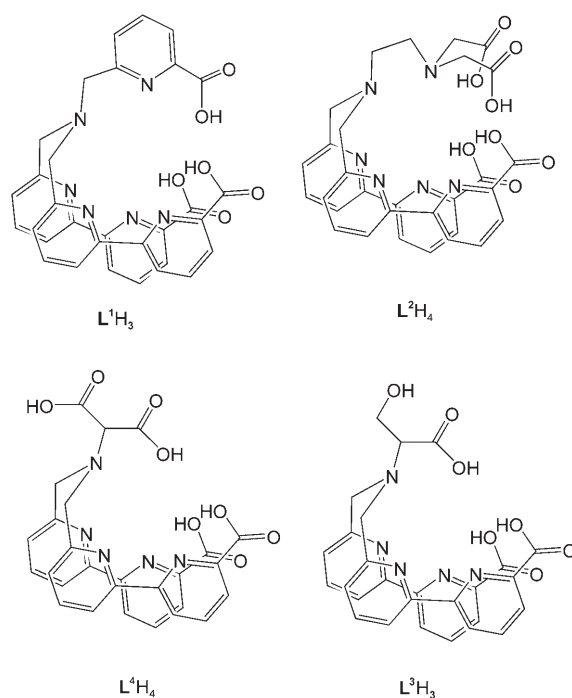


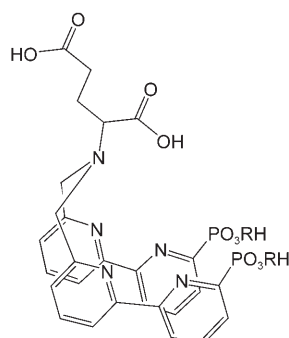
Figure 1. Three different coordination modes envisaged for $[Ln(L)(H_2O)]$.

nated by the two *N,N,O*-tridentate bipyridyl carboxylate arms (dark-grey strands in Figure 1), the central N_{glu} atom of the glutamate and its geminal carboxylate function coordinated by O_{glu} forming the third coordinating arm (light-grey strands in Figure 1). In coordination mode A, the bipyridyl arms (bipy) occupy equatorial positions in the complex. The water molecule is located at one pole of the molecule, opposite to the O_{glu} atom. In modes B and C, the bipy arms occupy all the lower sites of the complex and the water molecule is displaced at the upper part, next to the glutamate carboxylate strand. The difference between the two modes relies on the position of the water molecule relative to the glutamate. In mode B, H_2O is located in the plane defined by the lanthanide, N_{glu} and O_{glu} , and the water molecule and N_{glu} are placed symmetrically relative to the $Ln-O_{glu}$ axis. The plane containing N_{glu} , O_{glu} , Ln , and H_2O represents a pseudosymmetry plane in the complex. For mode C, the water molecule is nearly equidistant from N_{glu} and O_{glu} , disrupting the planar symmetry observed in mode B.

The synthetic strategies were then fitted to these three possible coordination modes in view of removing the water molecule. Mode B was the simplest case, as it consisted of elongating the glutamate strand by providing a ninth coordination site. Ligands **L¹** and **L²** were designed, in which the carboxylate function was replaced by a 2-aminomethylene-6-carboxy-pyridine or by an amino diacetate function. For mode C, the additional coordination site is provided by the introduction of a new coordination entity on the methylene bridging N_{glu} and O_{glu} species. This was achieved with ligands **L³** and **L⁴** in which the new coordination sites are a neutral hydroxymethylene or a negatively charged carboxylate function (at neutral pH in water), respectively. The hardest case to envisage was an A mode of coordination. The replace-



ment of the water molecule would require the introduction of a new strand on the ligand, necessitating total remodelling. Our approach was to increase the steric hindrance provided by the bipy arms. It has been shown previously that the replacement of carboxylate functions by phosphonate functions can increase steric hindrance in lanthanide complexes,^[14] thus resulting in a decrease of the coordination number and of the number of water molecules coordinated in the first sphere of the cation.^[15] Switching the bipyridyl carboxylate functions by phosphonate ones should lead to such an increased congestion and potentially to the removal of the water molecule (**L**⁵ and **L**⁶).



L⁵H₂ (R=Et); **L**⁶H₆ (R=H)

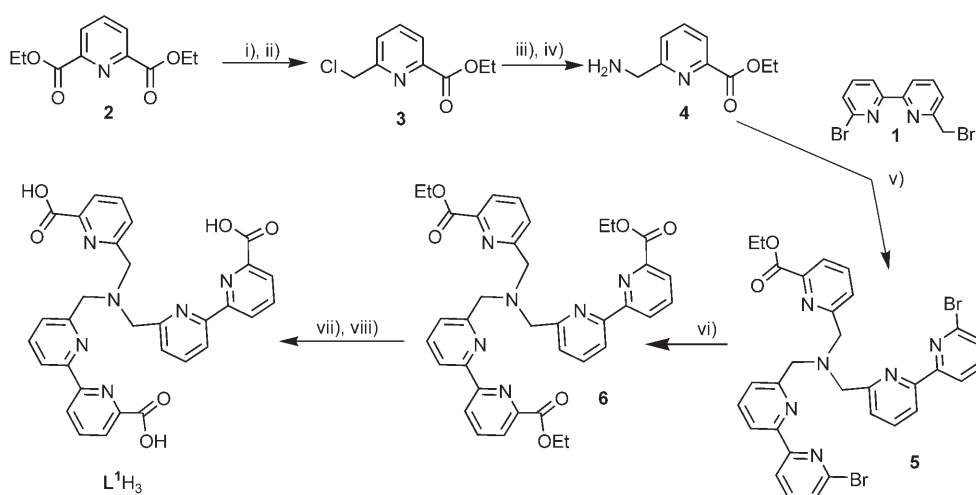
This work presents the synthesis of ligands **L**¹–**L**⁶, together with the formation of their lanthanide complexes with Eu and Tb and studies of their photophysical properties in water. A critical discussion of the relationship between the coordination ability of the ligands and potential removal of the water molecule is also presented.

Results and Discussion

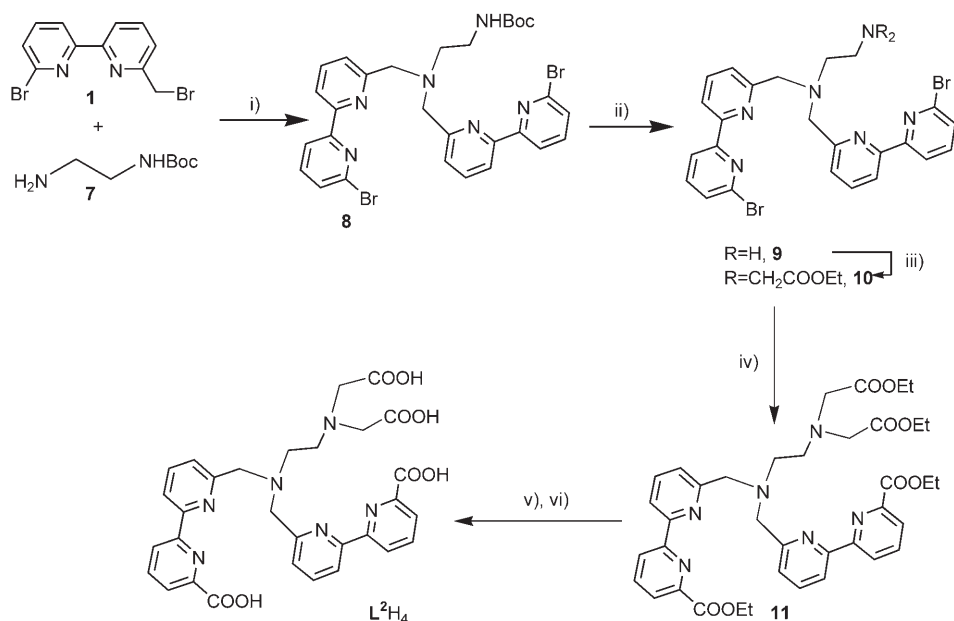
Synthesis of the ligands: Synthesis of ligands **L**¹–**L**⁶ relies on the key intermediate 6-bromo-6'-bromomethyl-2,2'-bipyridine (**1**; Scheme 1),^[16] which allows for the anchoring of the bipy arms on preorganised platforms through nucleophilic substitution at the bromomethylene position, while carboalkoxylation^[17] or phosphorylation^[18] reactions on the bromopyridine orthogonally permit the introduction of carboxylic or phosphonic acid functionalities.

Scheme 1 depicts the protocol for the synthesis of **L**¹. Starting from diethyl ester of dipicolinic acid (**2**), reduction with substoichiometric amounts of NaBH₄ affords the 6-hydroxymethyl-ethyl picolinic ester in 49% yield,^[19,20] which was transformed into the chlorinated compound **3** in 96% yield by treatment with SOCl₂.^[21] Amine **4** was obtained by a Gabriel synthesis by treating **3** with sodium phthalimide in DMF at room temperature (92%) followed by treatment with hydrazine in refluxing ethanol (quantitative).^[21] Nucleophilic substitution of **4** with **1** afforded the intermediate **5** in 67% yield, from which a carboalkoxylation reaction^[17] gave the ester precursor **6** in 45% yield. Saponification of **6** with NaOH followed by neutralisation with hydrochloric acid gave ligand **L**¹H₃ in 42% yield as its tetrahydrochloride salt.

The ligands **L**²–**L**⁴ were obtained by using similar protocols (Schemes 2 and 3). The ligand **L**²H₄ was obtained from the monoprotected ethylene diamine **7**,^[22] which gave the tertiary amine intermediate **8** in 47% yield upon condensation with **1**. Deprotection of the Boc group with TFA (92% yield) followed by reaction with ethylbromoacetate afforded the diester derivative **10** (68% yield). The sequence of carboalkoxylation, saponification, and neutralisation gave **L**²H₄ as its tetrahydrochloride salt with 59% yield for the three steps. Intermediate **11** could hardly be isolated in its pure form as a result of the presence of triphenylphosphine oxide



Scheme 1. i) NaBH₄ (0.6 equiv), EtOH, reflux (49%); ii) SOCl₂, 0°C (96%); iii) Na phthalimide, DMF, RT (92%); iv) H₂NNH₂·H₂O (3.5 equiv), EtOH, reflux (quant); v) **1** (2.2 equiv), K₂CO₃, CH₃CN, 80°C (67%); vi) [Pd(PPh₃)₂Cl₂] (cat), EtOH/Et₃N, CO (1 atm), 70°C (45%); vii) NaOH, MeOH/H₂O, 60°C; viii) 2N HCl (42% for the two steps).

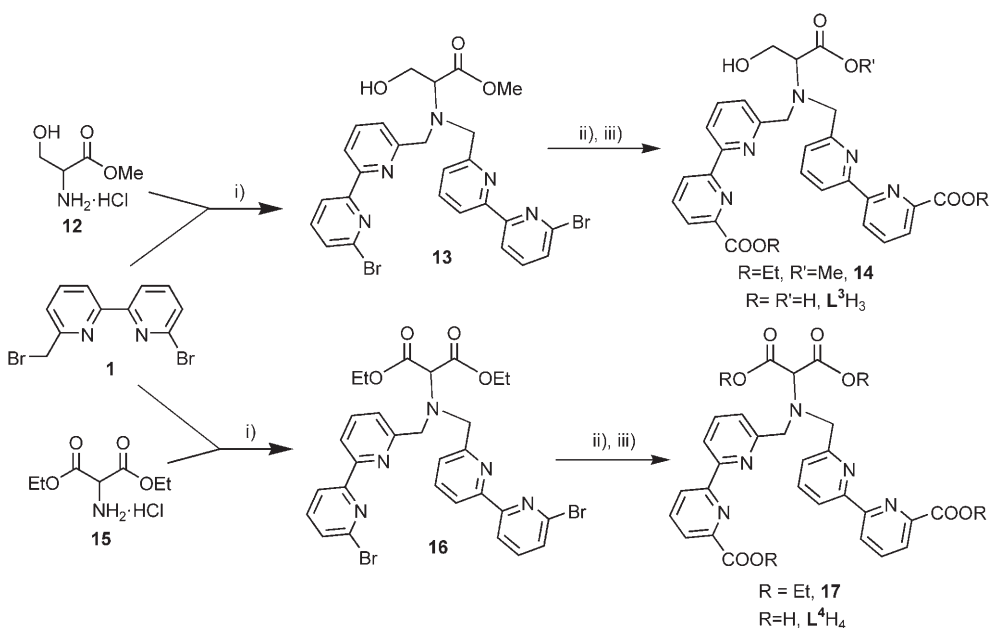


Scheme 2. i) Compound **1** (2.2 equiv), K_2CO_3 , CH_3CN , $80^\circ C$ (47%); ii) TFA, CH_2Cl_2 (92%); iii) ethyl bromoacetate (2.5 equiv), CH_3CN , K_2CO_3 , $80^\circ C$ (68%); iv) $[Pd(PPh_3)_2Cl_2]$ (cat), $EtOH/Et_3N$, CO (1 atm), $80^\circ C$; v) $NaOH$, $MeOH/H_2O$, $60^\circ C$; vi) $2N$ HCl (59% for the three steps).

formed during the carboalkoxylation reaction. Nevertheless, the lipophilic phosphine oxide can be easily removed from the reaction mixture after saponification.

Adapting the previous synthetic methodology, ligands L^3H_3 and L^4H_4 were obtained from the reaction of **1** and the hydrochloride salt of the methyl ester of serine (**12**) or the diethylester of aminomalonic acid (**15**) respectively, leading to compounds **13** (83%) and **16** in (56%), respectively

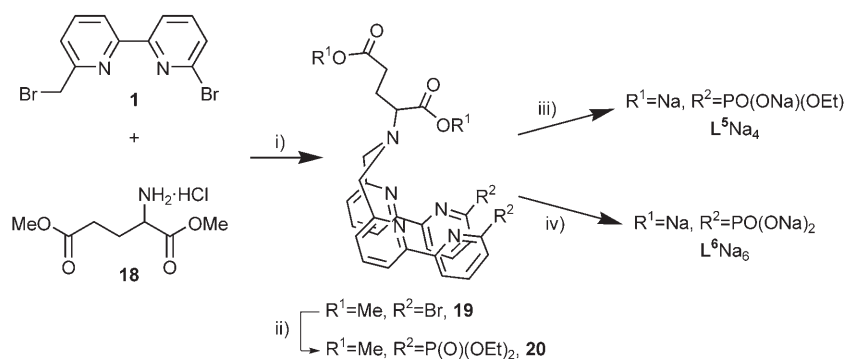
Two distinct hydrolysis routes were considered to obtain either ligand L^5 or L^6 . First, a saponification with sodium hydroxide in refluxing water led to the selective cleavage of one ethyl ester group of each phosphonate and to the hydrolysis of the carboxylic ester groups. Ligand L^5Na_4 was ultimately isolated with a good yield (79%) after precipitation in a water/THF mixture. Secondly, the hydrolysis of both phosphonic diester functions was possible due to trimethyl-



Scheme 3. i) K_2CO_3 , CH_3CN , $80^\circ C$ (83% for **12**, 56% for **15**); ii) $[Pd(PPh_3)_2Cl_2]$ (cat), $EtOH/Et_3N$, CO (1 atm), $80^\circ C$ (61% for **13**, 68% for **16**); iii) $NaOH$, $MeOH/H_2O$, $60^\circ C$; $2N$ HCl (82% and 53% for the two steps for L^3 and L^4 , respectively).

(Scheme 3). Carboalkoxylation of **13** and **16** gave the diesters **14** (61%) and **17** (68%), respectively, and saponification of the ester functions of **14** and **17** followed by acidification led to L^3H_3 in 82% yield and L^4H_4 in 53% yield, respectively, for the two steps).

Finally, as described during the synthesis of ligand **L**,^[11] the *N*-alkylation of the dimethyl ester glutamate hydrochloride salt **18** with slight excess of **1** led to compound **19** with a 67% yield (Scheme 4). A palladium(0)-catalysed step^[18] was used to introduce a diethyl phosphonate moiety in each 2,2'-bipyridine arm at the 6'-positions. The reaction was conducted in hot toluene containing diethylphosphite and Hünig's base to offer **20** in a 31% yield after purification.



Scheme 4. i) (2.2 equiv), CH_3CN , K_2CO_3 , 80°C , (67%);^[11] ii) $[\text{Pd}(\text{PPh}_3)_4]$ (cat), $\text{HPO}(\text{OEt})_2$, PPh_3 , toluene, $\text{N}(\text{iPr})_2\text{Et}$, 100°C , (31%); iii) 0.05 M aq NaOH , 100°C (79%); iv) TMSBr (29 equiv), $\text{CH}_2\text{Cl}_2/\text{CHCl}_3$, reflux; NaOH , H_2O , 80°C (71% for the two steps).

silyl bromide.^[18a,23] After evaporation of the solvent, a final saponification was performed to ensure that all the methyl esters were hydrolysed. Ligand L^6Na_6 was precipitated from a methanol/water mixture by adding THF, and obtained as its dihydrate with a 71% yield.

Photophysical studies of the ligands and complexes: For the purpose of clarity, the photophysical studies of the ligands and of their lanthanide complexes will be presented by order of increasing complexity rather than by numerical order.

Ligand L^5H_4 : The case of L^5 is clearly the simplest one as it was observed that it did not form stable complexes with the lanthanide cations in water solutions (0.01 M Tris/HCl, pH 7.0). This result is in line with prior results on the complexation of monoalkyl phosphonic esters functionalised at the 6-position of 2,2'-bipyridines,^[18b] which showed such tridentate units to be very weakly coordinating, in contrast to the corresponding phosphonic acid. For this reason, the photophysical properties of L^5 were not further investigated.

Ligand L^3H_3 : The behaviour of ligand L^3H_3 was easily understood as it is perfectly in line with previous results obtained with ligand LH_4 . Figure 2 displays the evolution of

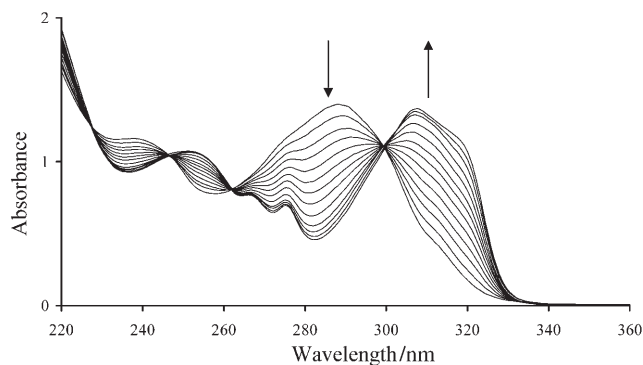


Figure 2. UV/Vis absorption spectra of a 5.6×10^{-5} M solution of L^3 in water (0.01 M Tris/HCl buffer, pH 7.0) titrated by $\text{EuCl}_3 \cdot 6\text{H}_2\text{O}$.

the UV-visible absorption spectra of a 5.6×10^{-5} M solution of L^3 (0.01 M Tris/HCl buffer, pH 7.0) upon addition of $\text{EuCl}_3 \cdot 6\text{H}_2\text{O}$. In water at neutral pH, the free ligand displayed two strong absorption bands at 238 and 288 nm, typical of the $\pi \rightarrow \pi^*$ transitions centred on the bipyridyl units in the *trans* conformation (Table 1).^[18b,24] Upon excitation in this absorption band, the emission spectra of the free

Table 1. UV/Vis absorption and emission data of the free ligands in water (0.01 M Tris/HCl buffer, pH 7.0).

	Absorption λ_{max} [nm] (ϵ [$\text{M}^{-1} \text{cm}^{-1}$])	Emission E [cm^{-1}]
L^1	240 (18700), 287 (22300)	25800
L^2	236 (14750), 288 (18400)	24650
L^3	238 (20700), 288 (24800)	24750
L^4	239 (20300), 288 (24800)	25800
L^6	237 (11400), 289 (14700)	24600
$\text{L}^{[11]}$	239 (20200), 288 (22300)	–

ligand in neutral buffered water displayed an intense emission band with a maximum at 404 nm (24750 cm^{-1}), which disappeared as soon as a delay time was enforced, pointing to a $^1\pi\pi^*$ state. Upon addition of up to one equivalent of the Eu^{III} ion (Figure 2), these transitions were bathochromically shifted to 251 and 308 nm, respectively, as a result of the *trans* to *cis* isomerisation of the bipyridyl fragments consecutive of the coordination of the cation. As expected, UV-visible spectrophotometric titration using $\text{TbCl}_3 \cdot 6\text{H}_2\text{O}$ displayed the same tendency, pointing to a 1:1 metal/ligand stoichiometry for the formed complexes.

The corresponding europium complex was obtained from a water/MeOH solvent mixture starting from equimolar amounts of the ligand and europium chloride salts. Interestingly, as long as the solution remained acidic, as a result of the introduction of L^3 in its protonated hydrochloric salt form, all species remain in solution, but the increase of the pH with diluted NaOH resulted in the formation of a precipitate. It is surmised that the different protonated forms of the complex are related to different coordination modes, as verified by the X-ray crystal structure of the complex obtained at low pH (see below). The elemental analysis and mass spectrum of the complex isolated at neutral pH pointed to a $[\text{Eu}(\text{L}^3)]$ formula. In dilute solution, the excitation of the complex into the bipyridyl-centred absorption bands led to the characteristic emission spectrum of europium, displaying the typical $^5\text{D}_0 \rightarrow ^7\text{F}_j$ ($J=0$ to 4) electronic transitions. Calculation of the relative intensities of the $^5\text{D}_0 \rightarrow ^7\text{F}_2/^5\text{D}_0 \rightarrow ^7\text{F}_1$ transitions indicated a low symmetry in the complex (as well as for all other Eu complexes described

herein, see Table T8, Supporting Information) and to the absence of an inversion centre in the coordination sphere. A weak fluorescence signal was observed around 400 nm, attributed to residual $^1\pi\pi^*$ emission and suggesting a partial energy transfer from the ligand to the metal. Photophysical data of the europium and terbium complexes (obtained from an equimolar solution of the ligand and Tb in the same solvent) are collected in Table 2.

Table 2. Photophysical data of the complexes in water (0.01 M Tris/HCl buffer, pH 7.0).

	λ_{max} [nm] (ϵ [$\text{M}^{-1} \text{cm}^{-1}$])	$\tau_{\text{H}_2\text{O}}$ ($\tau_{\text{D}_2\text{O}}$) [ms]	$\Phi_{\text{H}_2\text{O}}$ ($\Phi_{\text{D}_2\text{O}}$) [%]	$q^{[a]}$
L¹	Eu 273 (9500), 297 (9200), 321 (5100)	0.32 (2.18)	2.4 (2.8)	2.8 (2.9)
	Tb 272 (8500), 297 (9000), 318 (5200)	0.83 (1.78)	1.4 (2.1)	2.7 (2.9)
L²	Eu 247 (15850), 306 (18600)	1.12 (2.02)	9.5 (26)	0.1 (0.2)
	Tb 244 (13660), 305 (16000)	1.81 (1.92)	19 (32)	0.1 (0.1)
L³	Eu 251 (19000), 308 (24390)	0.57 (2.86)	4.4 (15)	1.2 (1.4)
	Tb 251 (19200), 307 (25500)	1.24 (1.98)	32 (51)	1.3 (1.2)
L⁴	Eu 252 (20700), 307 (23400)	0.57 (2.65)	4.4 (9.3)	1.2 (1.3)
	Tb 252 (20500), 306 (21000)	1.36 (1.87)	12 (35)	0.8 (0.7)
L⁶	Eu 250 (11600), 306 (14900)	0.58 (93%); 1.52 (7%), (2.89)	3.3 (17.2)	1.2 (1.4)
	Tb 251 (12100), 305 (15400)	1.03 (1.97)	3.5 (5.5)	1.9 (2.0)
L^[11]	Eu 253 (14400), 308 (19700)	0.62 (2.48)	8 (3.5)	1.1
	Tb 253 (15100), 308 (20800)	1.48 (2.53)	31 (53)	1.1

[a] Values in brackets correspond to those obtained according to Parker and co-workers,^[7b] see the Experimental Section for more details.

Luminescence decay lifetimes of the complexes in water and deuterated water were similar to complexes of **L**, although systematically smaller. From these data, it was possible to calculate the hydration number (q) corresponding to the number of water molecules directly coordinated into the first coordination sphere of the metal. Similarly to **L**, a hydration number of one was obtained for both complexes. Finally, the notable difference observed between the complexes of **L** and **L³** concerns the luminescence quantum yield of the europium complex, which appeared to be about twice as strong with **L** than with **L³** (Table 2). This behaviour can be explained by the proximity of the O–H oscillator provided by the serine alcohol function that brings additional deactivation pathways particularly sensitive in the case of europium. From these data, it can be estimated that the coordination geometry of **L³** must be rather similar to that of **L** and the introduction of a geminal hydroxymethyl function did not severely perturb the geometry of the coordination pocket at neutral pH.

Ligand L⁴H₄: The absorption spectrum of **L⁴H₄** in buffered water at pH 7.0 displayed the typical features of the bipyridinecarboxylate framework, as previously observed for **L³** and **L**, with the two intense $\pi \rightarrow \pi^*$ transitions, at 239 and 288 nm (Table 1). Upon excitation into these transitions the emission spectra displayed a broad emission band with maximum at 387 nm ($25\,800 \text{ cm}^{-1}$). The use of a 50 μs delay between excitation and integration of the emitted signal resulted in the loss of this band, which was attributed to the singlet $\pi\pi^*$ state centred on the bipyridyl unit. The coordination of europium or terbium cations led to the characteristic

bathochromic shift of the $\pi \rightarrow \pi^*$ transitions in the absorption spectra, found at 252 and 307 nm for Eu, and 252 and 306 nm for Tb. Upon excitation in the main absorption band (307 nm), both complexes exhibited emission spectra characteristic of their respective lanthanide cation, as a result of the ligand–metal energy transfer.^[6] The metal-centred luminescence was evidenced by the characteristic $^5\text{D}_1 \rightarrow ^7\text{F}_J$ transitions around 575, 595, 615, 655 and 690 nm for Eu ($I=0, J=0$ to 4) and around 495, 545, 585 and 620 nm for Tb ($I=4, J=6$ to 3). Interestingly, no residual fluorescence could be observed, indicating a very efficient ligand–metal energy transfer. Recording the excitation spectra with emission monitored on the most intense emission band of the lanthanide cations ($^5\text{D}_0 \rightarrow ^7\text{F}_2$ at 617 nm for Eu and $^5\text{D}_4 \rightarrow ^7\text{F}_5$ at 546 nm for Tb) afforded a perfect match with the corresponding absorption spectra, thereby unambiguously confirming the antenna effect. Luminescence lifetime measurements in water and D₂O

(Table 2) allowed for the calculation of the hydration number, $q=1.2^{[7c]}$ or $1.3^{[7b]}$ in line with the coordination of a single carboxylate function of the malonic moiety. Comparison of the luminescence lifetimes for **L⁴** and **L** (Table 2) pointed to a more pronounced deactivating effect due to solvation for **L⁴**. This is translated into a slightly higher hydration number for **L⁴** compared to **L** ($q=1.1$) that may be attributed to second-sphere interactions possibly arising from the replacement of the alkyl chain in **L** with a more hydrophilic carboxylate function in **L⁴**. The higher activity of deactivating O–H oscillators is also reflected into smaller luminescence quantum yields for **L⁴**. Finally, the introduction of a geminal carboxylate function on the amine did not displace the water molecule from the first coordination sphere, which suggests that coordination mode C is not effective in this case.

Ligand L¹H₃: The UV-visible absorption spectrum of **L¹H₃** (Figure 3, Table 1) in buffered water at pH 7.0 (0.01 M Tris/HCl) is slightly different from those observed for **L³** and **L⁴**. An intense absorption band is still present with maximum at 287 nm (Table 1), but it is far broader, particularly in the 270–280 nm region, compared to ligands lacking the pyridine carboxylate moiety (Figure 2). This enlarged absorption is ascribed to the combination of the $\pi \rightarrow \pi^*$ absorption band of the bipyridyl moieties at 288 nm, together with the weaker $\pi \rightarrow \pi^*$ transition centred on the pyridyl carboxylate subunit, with the maximum peaking at 268 nm as observed in compounds containing the pyridine–carboxylate chromophore.^[26] Upon excitation in the UV domain, the emission spectrum displayed a broad emission band with maximum at

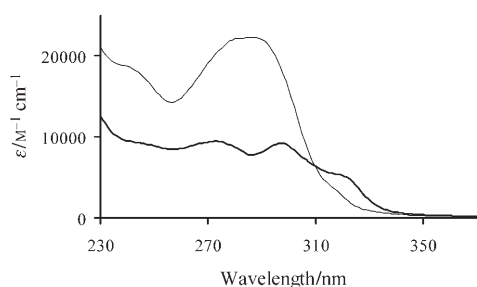


Figure 3. UV/Vis absorption spectra of L^1 (normal line) and its europium complex (bold line) in water (0.01 M Tris/HCl buffer, pH 7.0).

387 nm (25800 cm^{-1}), which is attributed to the ${}^1\pi\pi^*$ state of the bipyridyl units, in agreement with what was previously observed for L^3 , L^4 , and L . No additional emission arising from the pyridine ring could be observed.

The absorption spectra of the Eu and Tb complexes of ligand L^1 (Figure 3) are very different from those previously observed (see, for example, Figure 2). They both display three main bands at 321, 297 and 273 nm for Eu and 318, 297 and 272 nm for Tb. Upon coordination of the lanthanide cations, the $\pi\rightarrow\pi^*$ transitions are not as significantly displaced toward lower energy as previously observed (down to 308 nm for example for L and L^3 , Figure 2). The spectra better reflect the superimposition of two distinct bands. While the former band, displaying a shoulder at low energy (320 nm), could be attributed to a coordinated bipyridine-carboxylate arm, the latter band (at 297 nm) reflected an intermediate situation, in which the bipyridine is neither directly coordinated ($\lambda_{\text{max}}=308\text{ nm}$) nor free ($\lambda_{\text{max}}=288\text{ nm}$). The bathochromic shift observed in comparison to the free ligand points to a conformational change in which the *trans* conformation, observed for the free ligand and due to the nitrogen lone-pair repulsion,^[18b,24] is replaced by a conformation having a pronounced *cis* character. Similar behaviour has already been observed in bipyridine containing lanthanide complexes^[25] and was understood to be second-sphere interactions mediated by bridging water molecules. A large hypochromic effect is concomitantly observed upon complexation, in agreement with a spreading of the absorption bands. Upon excitation in the ligand absorption bands, the complexes displayed emission spectra typical of their corresponding lanthanide cations, with no residual fluorescence from the ligand, pointing to an efficient ligand-metal energy-transfer process. The corresponding excitation spectra are in excellent agreement with the absorption spectra, which indicates that even if one bipyridyl arm is not coordinated, it efficiently transfers its energy to the cation. Furthermore, this almost perfect superimposition also points to the efficient sensitisation from the pyridyl carboxylate subunit of the ligand, as previously suggested.^[26] Surprisingly, the measured luminescence quantum yields were particularly weak (Table 2). In parallel, the excited-state lifetimes measured for both Eu and Tb were significantly smaller than those observed for other ligands or for L (Table 2).

The calculations of the hydration numbers^[27] appeared particularly informative. For both Eu and Tb, a hydration number close to three was obtained, in complete contradiction with the increased denticity afforded by the ligand. On the basis of an N-podand-type structure, a nonacoordination was expected for L^1 , which was supposed to remove all the water molecules from the first coordination sphere. However, addition of the pyridyl carboxylate functions resulted in a total change of the coordination mode, as preliminarily suggested by the absorption data. Prior experiments made on a ligand composed of an *N*-butyl amine functionalised by two bipyridyl carboxylate arms showed that the emergent lanthanide complexes contained two water molecules in the first coordination sphere.^[27] The presence of three water molecules can hardly be explained, but could arise from the decoordination of one bipyridyl arm concomitantly to the coordination of the pyridyl one. The coordination of the central nitrogen atom, the N-O bidentate fragment of the pyridyl carboxylate function and of the N-N-O tridentate fragment of a bipyridyl carboxylate would lead to a hexadenticity that should explain the presence of three water molecules coordinated to the cation. This should also explain the observed results of absorption experiments that pointed to one coordinated bipyridyl, the second one being relegated to second-sphere interactions. Different reasons for the decomplexation of one bipyridyl strand can be postulated. The first is that the wrapping of the three heterocyclic moieties around the cation is disfavored by steric congestion at the central nitrogen atom. Prior results on the complexation of lanthanide cations with podand-type ligands such as α,α',α'' -nitriolo-(6-methyl-2-pyridinecarboxylic acid) (tpaaH₃) showed that the wrapping is perfectly feasible with short coordination arms such as pyridyl carboxylate.^[28] More probably, the introduction of one supplementary pyridine group on two coordinating arms led to steric hindrance opposite to the nitrogen node, resulting in the preferred decoordination of one bipyridyl arm in favour of the pyridine tether.

Ligand L^2H_4 : The UV-visible absorption spectrum of ligand L^2H_4 in neutral buffered water (Figure 4) displayed absorption bands at 288 and 236 nm ($\epsilon=18400$ and $14750\text{ M}^{-1}\text{ cm}^{-1}$, respectively), attributed to the $\pi\rightarrow\pi^*$ transitions centred on the bipyridyl units. Excitation into this transition (288 nm) led to a large emission band with a maximum at 406 nm (24650 cm^{-1}), attributed to the ${}^1\pi\pi^*$ emission, on the basis of its short-lived character.

In contrast to what was previously observed for L^3 (Figure 2) or L , the UV-visible titration of L^2 by $TbCl_3$ in water clearly showed the absence of isosbestic points, pointing to the presence of at least two new absorbing species formed during the titration. Careful examination of the evolution of the absorbances at fixed wavelengths suggested the successive formation of species with $[M(L^2)_2]$ and $[M(L^2)]$ formulations.

Eu and Tb complexes were isolated from methanol/water mixtures, each containing equimolar amounts of the ligands in their acidic forms and the corresponding lanthanide chlo-

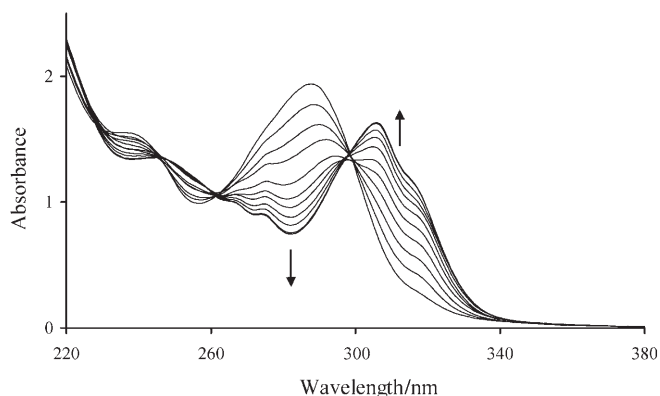


Figure 4. Evolution of the UV/Vis absorption spectra of a 1.05×10^{-4} M solution of L^2H_6 in water (0.01 M Tris/HCl buffer, pH 7.0) upon addition of 0.11, 0.22, 0.33, 0.44, 0.55, 0.66, 0.77, 0.88, 1.0, and 1.22 equiv of $TbCl_3 \cdot 6H_2O$.

ride salts. After heating to $60^\circ C$ for a few hours, allowing for formation of the thermodynamically stable species, the solutions were cooled and the pH raised to 8–9 with Et_3N to neutralise the excess of protons and to generate a strong complexation with the carboxylate functions. Concentration of the solutions followed by addition of Et_2O resulted in the precipitation of white powders, displaying the typical luminescence of the corresponding lanthanide ions upon UV irradiation. Elemental analysis of the powders pointed to a general formulation with a 1:1 metal/ligand ratio, together with the presence of a triethylammonium cation, $(Et_3NH)[Ln(L^2)]$. Finally, mass spectrometry of the europium complex by using FAB in the negative detection mode showed the main peak as being due to a $[Eu(L^2)]^-$ species. Figure 5 displays the absorption, excitation, and emission spectra of the europium complex. As expected on the basis of the titration, the $\pi \rightarrow \pi^*$ absorption bands centred on the bipyridyl units were bathochromically shifted upon complexation, but in contrast to what was observed for L^3 (Figure 2) or L , the absorption band is less shifted (306 nm compared to 308 nm for L^3 and L) and the band appears thinner. For

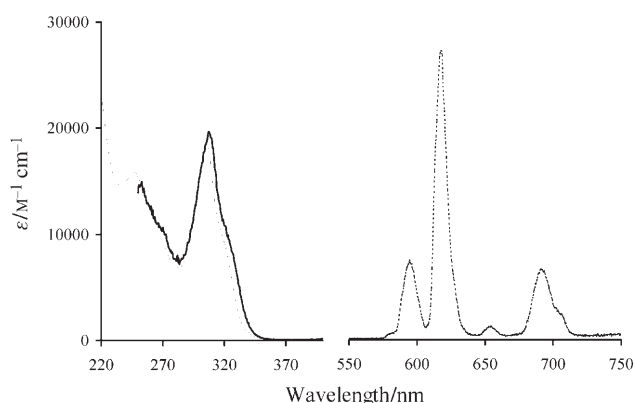


Figure 5. UV/Vis absorption (thin line), excitation (bold line), and emission (dotted line) spectra of $(Et_3NH)[Eu(L^2)]$ in water (0.01 M Tris/HCl buffer, pH 7.0).

L^3 and L , the intensities ratio at 308 and 320 nm was very close to unity (1.1), whereas in the case of L^2 , this ratio approached a value of 2.0. The shape of the band suggests a *cis* configuration of the bipyridyl units, but a weakened coordination of these arms. Upon excitation in the $\pi \rightarrow \pi^*$ absorption bands, the typical emission of Eu is observed, with no remaining emission from the ligand, and the excitation spectrum obtained upon monitoring the europium emission is almost perfectly superimposable to the absorption spectrum, suggesting an efficient energy-transfer process.

The photophysical data of the Eu and Tb complexes are gathered in Table 2. They showed the two complexes to be highly luminescent in water, the europium complex of L^2 being even more luminescent than the complex of L (9.5 and 8% overall quantum yield, respectively). In all cases, the metal-centred luminescence decays were perfectly monoexponential, indicative of the presence of single-emitting species in solution. A striking point concerns the calculation of the hydration number. For both complexes, luminescence lifetime values obtained in H_2O and D_2O showed that no water molecules were bonded to the cations. The perfect filling of the first coordination sphere is clearly in favour of a coordination mode of type B (Figure 1), in which the lengthening of the upper coordinating arm allows for displacement of the water molecule. Nevertheless, the energy and shape of the absorption band of the complex suggest a weakened coordination of the bipyridyl arms, which may result from the introduction of the fourth carboxylate function. This additional coordinating arm may induce a large change in the coordination mode of the ligand, possibly acting as a decatate ligand, strengthened by electrostatic interactions with the triethylammonium cation^[26a] or by a so-called “clipping effect”.^[29]

Ligand L^6H_6 : The UV-visible absorption spectrum of ligand L^6 in water (0.01 M Tris/HCl buffer, pH 7.0) is presented in Figure 6, and displayed the characteristic $\pi \rightarrow \pi^*$ transitions centred on the bipyridyl units at 237 and 289 nm (Table 1). In addition, a pronounced shoulder can be observed around 315 nm. The pK value for the second deprotonation of bipyridyl-functionalised phosphonic acid was determined to be 7.1,^[18b] and at pH 7.0 the mono- and fully deprotonated forms of phosphonic acid coexist. In the monodeprotonated form, the $\pi \rightarrow \pi^*$ transitions have been shown to be batho-

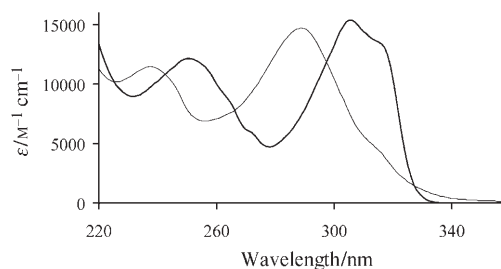


Figure 6. UV/Vis absorption spectra of L^6H_6 (normal line) and its Eu complex (bold line) in water (0.01 M Tris/HCl buffer, pH 7.0).

chromically shifted,^[18b] and are probably the cause of the 320 nm shoulder. Upon excitation in the maximum of the absorption band, a large emission band can be observed with maximum at 406 nm (24600 cm^{-1}), attributed to the $^1\pi\pi^*$ on the basis of its short-lived character.

The absorption spectra of the Eu (Figure 6) and Tb complexes (Table 2) showed the typical bathochromic shift of the $\pi\rightarrow\pi^*$ absorption bands observed upon complexation of the lanthanides. Excitation in this absorption band (304 nm) revealed emission features characteristic of the Eu and Tb cations and evidenced an effective ligand-to-metal sensitisation process. Surprisingly, the overall quantum yield measured for metal-centred luminescence upon ligand excitation appeared very low for both complexes, when compared to the reference complexes of **L**. Finally, the measurements of luminescence decay lifetimes revealed differences between europium and terbium. For Eu, a biexponential decay was observed in water with a main component (93%) for the shortest-lived species, with a luminescence decay lifetime of 0.58 ms, similar to those measured for **L**, **L**³ and **L**⁴. A longer component ($\tau=1.52\text{ ms}$) was observed amounting to 7% of the total luminescence. In deuterated water, the luminescence decay was perfectly monoexponential and by using this value it was possible to calculate that the short-lived species has an average hydration number of 1.5, whereas the long-lived one contains no coordinated water molecules. Among possible explanations for the presence of this latter species, one arose from the possibility of intermolecular interactions in which phosphonate functions bridge two lanthanide cations, as was observed for Eu and Yb complexes with the anion of 6-phosphonic-2,2'-bipyridine acid in the solid state.^[30] For Tb, the calculation led to a hydration number of two. Such elevated values of q suggest that **L**⁶ is acting as a heptadentate ligand. This statement agrees with the fact that the formal “-4” charge brought by the phosphonate functions largely counterbalances the positive charge of the lanthanide cations and this polarisation destabilises the interaction with the carboxylate function, possibly disrupting it. A rapid kinetic equilibrium between species with a bonded or a free carboxylate would result in average hydration numbers of between one and two.

X-ray crystal structure of [Eu(L³H₂)Cl]Cl·3H₂O: Single crystals of [Eu(L³H₂)Cl]Cl·3H₂O were obtained by slow concentration of a solution containing equimolar amounts of L³H₃·4HCl and EuCl₃·6H₂O in water. The crystal structure of the complex (Figure 7) shows it to be composed of a europium cation coordinated by a monodeprotonated L³H₂⁻ ligand and a chloride anion. The charge of the resulting [Eu(L³H₂)Cl]⁺ complex is compensated by an uncoordinated chloride anion. Three water molecules of solvation complete the content of the crystallographic asymmetric unit.

In the complex, the ligand reveals very interesting features. In particular, L³H₂⁻ is coordinated to the europium ion through the central nitrogen atom of the serine moiety and the bipyridyl arms are wrapped around the cation in a single-stranded mononuclear helical arrangement,^[31] allow-

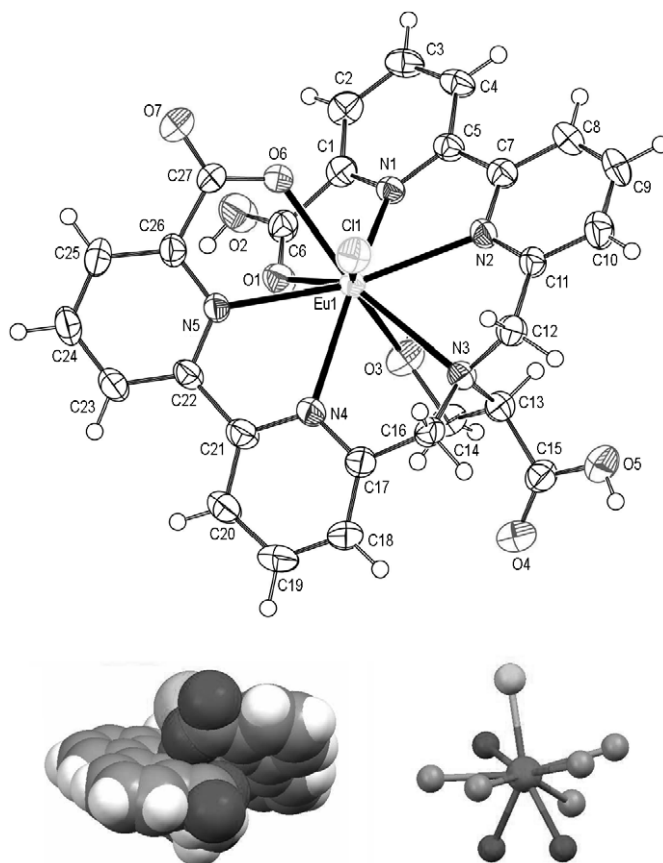


Figure 7. ORTEP view of complex [Eu(L³H₂)Cl]⁺ (top). Representation of the europium coordination sphere showing the helical wrapping of the ligand (bottom left) and the coordination polyhedron around europium (bottom right).

ing the coordination of the four nitrogen atoms of the bipyridyl strands and of the oxygen atoms of the carboxylic acid functions. The bipyridyl-carboxylate frames are almost planar with dihedral angles of 8.6 and 4.6° around the C–C bond that links the pyridyl rings, and 16.4 and 4.6° for the dihedral angles around the C–C bond that links the external pyridyl ring and the carboxylic functions. The helical wrapping of this heptadentate part results in more than one turn, so that the carboxylic acid functions are placed one above the other. As a result of the acidic conditions of crystallisation, only a single bipyridyl carboxylic function was deprotonated, which resulted in two distinct Eu–O distances of 2.390 and 2.520 Å, respectively, for the deprotonated and protonated oxygen atoms. The Eu–N distances of the pyridyl rings are, on average, 2.56 Å, corresponding to typical values for this type of ligand.^[32,33] The remaining two coordination sites of the nonacoordinated europium atom are positioned on opposite sites from the plane perpendicular to the helical axis. They are occupied by a chloride anion and by the alkoxy residue of the serine moiety. Surprisingly, the imposed acidic conditions led to the protonated carboxylic acid function and, in that case, a coordination of the alcohol was preferred to that of the protonated acid.

The three-dimensional framework crystal structure results from a combination of a cooperative hydrogen-bond network (Table T7, in the Supporting Information) and π stacking interactions (Figure 8). The three water molecules link

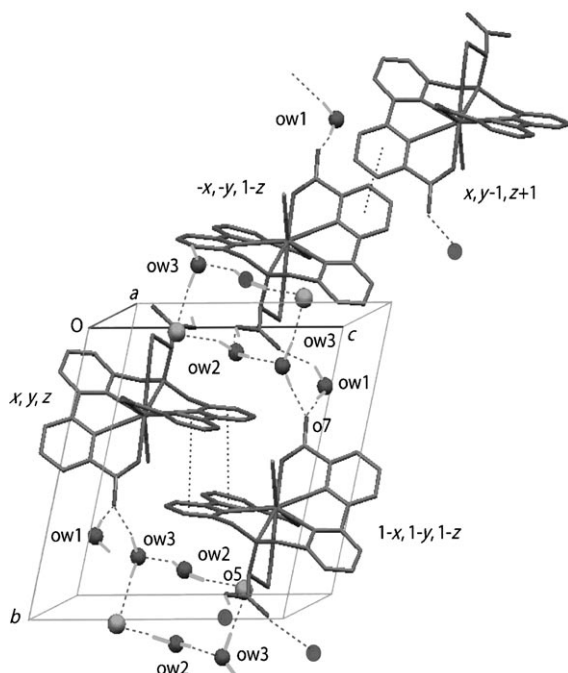


Figure 8. Three-dimensional packing of $[\text{Eu}(\text{L}^3\text{H}_2)\text{Cl}]\text{Cl}\cdot 3\text{H}_2\text{O}$.

the protonated O5 atom from the carboxylate function of a $[\text{Eu}(\text{L}^3\text{H}_2)\text{Cl}]^+$ molecule at (x, y, z) to the unprotonated O7 atom of a molecule at $(1-x, 1-y, -z)$ in a cooperative hydrogen-bond network to form a layer structure parallel to the $-ab$ plane (Figure S1, in the Supporting Information). The hydrogen-bond ring pattern formed is of graph set $\text{R}_5^4(8)$.^[34] The stabilisation is increased by a single π - π stacking interaction. The N5 pyridyl rings in the molecule at (x, y, z) and $(-x, 1-y, -z)$ are strictly parallel, with an interplanar spacing of $3.443(3)$ Å; the ring-centroid separation is $3.665(3)$ Å, corresponding to a ring offset of $1.103(3)$ Å. Among the three water molecules, OW2 and OW3 are involved with the chloride anion Cl2 in a hydrogen-bond pattern of graph set $\text{R}_6^4(12)$ that runs along the b -axis direction, alternately with the N1-N2 bipyridyl groups in the molecule at (x, y, z) and $(1-x, 1-y, 1-z)$ in weak π - π stacking interaction (minimum centroid separation $4.013(3)$ Å; minimum interplanar spacing of $3.225(3)$ Å).

It is worth noting that if the pH of the mother solution was raised above 4 by addition of diluted NaOH, a white precipitate formed affording the $[\text{Eu}(\text{L}^3)(\text{H}_2\text{O})]$ neutral complex. The deprotonation of the carboxylic acid functions resulting from the pH increase is suspected to generate a rearrangement in the coordination mode. A simple rotation around the C-N bond of the serine core will lead to a preferred coordination of the carboxylate function. This is con-

firmed by FTIR studies in the solid state displaying a sharp band at 1737 cm^{-1} in the spectrum for the protonated carboxylic acid of $[\text{Eu}(\text{L}^3\text{H}_2)\text{Cl}]\text{Cl}$, which disappeared in the spectrum of $[\text{Eu}(\text{L}^3)(\text{H}_2\text{O})]$. Finally, deprotonation of the second bipyridyl arm, with a pK value in the 4–5 range,^[18b] will compensate the overall charge of the cation, weakening the Eu-Cl bond, and resulting in its facile decoordination and replacement by a water molecule. According to this X-ray crystal structure, a coordination mode of type A is reasonably envisaged.

Conclusion

On the basis of simple convergent synthetic strategies, we have developed a family of multitopic ligands for the coordination of lanthanide cations. All these ligands carry two bipyridine subunits functionalised with carboxylate or phosphate anionic functions. The corresponding europium and terbium complexes are all luminescent in water at neutral pH and their photophysical characteristics can be finely interpreted within the frame of a structure-property relationship.

The various changes made in comparison with the reference complexes of **L** (glutamate) allowed us to draw the following conclusions. From the complexation behaviour of ligand **L**³ (serine) and **L**⁴ (aminomalonate), it clearly appeared that the coordination mode C can be disregarded. In both cases, hydration numbers and absorption data suggest complexation trends similar to that of **L** and the additional geminal coordinating arms notably influence the relative efficiencies of luminescence, providing supplementary radiative deactivation pathways. Replacing bipyridyl carboxylic acid functions by phosphonic functions had the opposite effect to the one expected. While it was hoped that the bulkier phosphonic functions should sterically hinder the complexation of the coordinated water molecules,^[14,15] it resulted in a weakened coordination of the carboxylate moiety opening the coordination shell to even more water molecules. Finally, the approach consisting of the elongation of the glutamic coordinating arm showed contrasting results. Elongation through the addition of a supplementary pyridyl ring led to the decoordination of one bipyridyl strand, allowing the access of three water molecules. The elongation through addition of an aminodiacetate function was finally successful, leading to the displacement of the water molecule and the perfect filling of the coordination sphere. It is nevertheless not clear whether this is the proof of a coordination mode of type B, or, as suggested by the absorption data, it arose from a change in the coordination mode with a potential decadentate coordination mode. Last but not least, a better insight into the coordination mode was probably gained through the methodology that first failed and engendered this study. X-ray diffraction analysis on single crystals of the europium complex of **L**³ (serine) revealed a wrapping of the two bipyridylcarboxylate arms that did not leave much room for another coordination mode other than the A type.

This last result unfortunately points to great difficulties in trying to remove the coordinated water molecule by a judicious ligand design. Even when the coordination sphere could be completed, the photophysical improvements brought about by the removal of the water molecule remained largely modest compared to the synthetic efforts devoted to their preparation.

Experimental Section

Materials and methods: Column chromatography and flash column chromatography were performed by using silica (0.063–0.200 mm, Merck) or silica gel (40–63 µm, Merck) or on standardised aluminium oxide (Merck, Activity II-III). Acetonitrile was filtered over aluminium oxide and distilled over P₂O₅, DMF was distilled under reduced pressure and diisopropylethylamine was refluxed over KOH and distilled prior to use. Other solvents were used as purchased. Melting points were measured by using a Büchi Melting Point 535 apparatus and are uncorrected. ¹H and ¹³C NMR spectra were recorded on Bruker AC 200, Avance 300 and Avance 400 spectrometers working at 200, 300 or 400 MHz, respectively. ³¹P (162 MHz) spectra were obtained by using the Bruker Avance 400 spectrometer, implemented with internal calibration mode. Chemical shifts are given in ppm, relative to the residual protonated solvent.^[35] IR spectra were recorded by using a Nicolet 210 spectrometer as KBr pellets. Compounds **1**,^[16] **3**,^[20] **4**^[21] and **7**^[22] were obtained according to literature procedures and full experimental procedures for the synthesis of intermediate compounds **5**, **6**, **8**, **9**, **10**, **13**, **14**, **16**, **17**, and **20** are reported in the Supporting Information.

Absorption and emission spectroscopy: UV/Vis absorption spectra were recorded on a Uvikon 933 spectrometer. Emission and excitation spectra were recorded on a Perkin–Elmer LS50B (working in the phosphorescence mode) or a PTI Quantmaster spectrometer. When necessary (Eu complexes) a Hamamatsu R928 photomultiplier was used. Luminescence decays were obtained on the PTI Quantmaster instrument over temporal windows covering at least five decay times. Luminescence quantum yields were measured according to conventional procedures,^[36] with diluted solutions (optical density < 0.05), by using [Ru(bipy)₃]Cl₂ in nonde-gassed water ($\Phi = 2.8\%$)^[37] or rhodamine 6G in ethanol ($\Phi = 88\%$)^[38] as references, with the necessary correction for refractive index of the media used.^[39] Estimated errors are ± 15%. Photophysical measurements were obtained on isolated complexes for ligands **L**¹ and **L**², and on solutions containing equimolar amounts of ligand and lanthanide chloride in the other cases. Spectrophotometric titrations were performed according to a previously published procedure.^[27b] Hydration numbers (*q*) were obtained by using Equation (1), in which $\tau_{\text{H}_2\text{O}}$ and $\tau_{\text{D}_2\text{O}}$ refers to the measured luminescence decay lifetime (in ms) in water (0.01 M Tris/HCl buffer, pH 7.0) or deuterated water (after evaporation of water, drying under vacuum, and dissolution in D₂O), respectively, by using $A = 1.11$ and $B = 0.31$,^[7c] or $A = 1.2$ and $B = 0.25$,^[7b] respectively, for Eu, and $A = 5$ and $B = 0.06$,^[7b] or $A = 4.2$ and $B = 0$,^[7a] respectively, for Tb (estimated error ± 0.2 water molecules).

$$q = A \times (1/\tau_{\text{H}_2\text{O}} - 1/\tau_{\text{D}_2\text{O}} - B) \quad (1)$$

X-ray crystallography: Room-temperature data collection was from a thick plate-type, air-sensitive crystal mounted inside a sealed Lindemann capillary on an Enraf–Nonius Kappa-CCD diffractometer by using graphite-monochromated MoK α ($\lambda = 0.71073$ Å) radiation. A preliminary orientation matrix and unit cell parameters were determined from a ϕ scan of 10° with 20 s deg⁻¹ of oscillation, followed by spot integration and least-squares refinement.^[40,41] The strategy^[40,41] for complete data collection in the triclinic system suggested a ϕ scan of 183° range with a 1.8° oscillation, followed by three ω scans of successive lengths: 47.3, 57.8 and 60.1°. “Dezincering” was accomplished by measuring each frame twice with 45 s exposure per degree. The detector was put at the position of 40 mm.

Data reduction and cell-dimension post-refinement were performed by using the HKL2000 package.^[41] Correction for absorption mainly due to Eu atoms was used as implemented within SCALEPACK.^[41] The structure was solved by using the PATTERSON method (SHELXS-97)^[42] and all non-hydrogen atoms were refined with anisotropic displacement parameters by using SHELXL-97^[42] by full-matrix least-squares on F^2 values. All hydrogen atoms were located in difference Fourier maps, but a riding model was used with $U_{\text{iso}}(\text{H})$ set at 1.2 U_{eq} of the attached atom for all them except the hydrogen atoms of the water molecules for which the positional parameters were freely refined, but their $U_{\text{iso}}(\text{H})$ values set at 1.5 $U_{\text{eq}}(\text{O})$.

Crystal data for [Eu(L³H₂)Cl]Cl·3H₂O: [C₂₇H₂₈Cl₂EuN₅O₁₀], $M_r = 805.40$ g mol⁻¹, plate crystal size 0.125 × 0.38 × 0.42 mm, triclinic, space group $P\bar{1}$, $a = 10.002(1)$, $b = 12.793(1)$, $c = 13.012(1)$ Å, $\alpha = 99.960(6)$, $\beta = 96.173(6)$, $\gamma = 106.178(3)^\circ$, $V = 1553.5(2)$ Å³, $Z = 2$, $\lambda = 0.7107$ Å, $F(000) = 804$, $\mu = 2.254$ mm⁻¹, $T = 293(2)$ K, $\rho_{\text{calcd}} = 1.722$ mg m⁻³, 11 750 data measured of which 5981 unique ($R_{\text{int}} = 0.0324$) and 5979 observed with $I > 2\sigma(I)$, Completeness to $\theta_{\text{max}} = 98.0\%$, 426 parameters with no restraints, $wR_2 = 0.1025$, $S = 1.051$, $R_1 = 0.0468$ (all data), final difference max peak/hole = 1.144/–1.824 e Å⁻³.

CCDC-611675 contains the supplementary crystallographic data for this paper, these data can be obtained free of charge from the Cambridge Crystallographic Data Centre via www.ccdc.cam.ac.uk/data_request/cif.

Crystal data and selected experimental details, list of atomic coordinates, bond lengths and angles, anisotropic thermal parameters of non-hydrogen atoms, atomic coordinates of hydrogen atoms are reported in the Supporting Information.

Preparation of ligand L¹H₃·4HCl: A solution of **6** (182 mg, 0.28 mmol) and NaOH (66 mg, 1.65 mmol) in a mixture of methanol (18 mL) and water (5 mL) was heated to 60 °C for 17 h. The solution was evaporated to dryness and the resulting solid was dissolved in water (10 mL). Aqueous HCl (2 N) was slowly added until a precipitate appeared. After centrifugation, the product was dissolved in methanol, filtered over Celite and evaporated. L¹H₃·4HCl (83 mg, 42%) was isolated as a white powder. ¹H NMR (D₂O/tBuOH, 200 MHz): $\delta = 3.63$ (s, 4H), 3.83 (s, 2H), 7.16 (d, ³ $J = 7.5$ Hz, 2H), 7.41–7.53 (m, 3H), 7.64–7.72 (m, 8H), 7.79–7.83 ppm (m, 2H); IR (KBr): $\tilde{\nu} = 3420$ (s), 3085 (m), 2921 (m), 2846 (m), 1723 (m, C=O), 1620 (m, COO_{asym}), 1584 (m, COO_{asym}), 1444 (m), 1384 (m, COO_{sym}), 1345 (m), 1302 (m), 1258 (m), 1076 cm⁻¹ (w); UV/Vis (0.01 M Tris/HCl buffer, pH 7.0): $\lambda_{\text{max}} (\epsilon_{\text{max}}) = 240$ (18700), 287 nm (22300); MS (FAB⁺): m/z (%): 577.3 (30) [L¹H₃+H]⁺; elemental analysis calcd (%) for C₃₁H₂₈N₆O₈·4HCl: C 51.54, H 3.91, N 11.63; found: C 51.46, H 4.28, N 11.49.

Preparation of ligand L²H₄·4HCl·2H₂O: Compound **10** (210 mg, 0.29 mmol) was heated at 80 °C in a solution of [Pd(PPh₃)₂Cl₂] (20 mg, 29 µmol) in Et₃N/EtOH (10 mL each) as catalyst under a continuous flow of CO gas. After 16 h, a second portion of catalyst (20 mg, 29 µmol) was added and the heating and bubbling continued for another 16 h. After cooling, the solution was evaporated to dryness and the residue was dissolved in CH₂Cl₂, filtered over cellulose and evaporated again to dryness. The remaining residue was purified by column chromatography (SiO₂, CH₂Cl₂/MeOH, 100:0 to 96:4) to afford the tetraester **11** containing triethylammonium bromide and Ph₃PO as impurities ($R_f = 0.60$, SiO₂, CH₂Cl₂/MeOH, 80:20). The solid was dissolved in MeOH (10 mL) and NaOH (214 mg, 5.3 mmol) in H₂O (3 mL) was added. The solution was heated for 3 h at 60 °C. The pH of the solution was raised to 2 with concd HCl, the solution was evaporated to dryness, and the residue was dissolved in MeOH. Addition of THF resulted in precipitation of a voluminous white solid (NaCl), which was filtered. After evaporation of to dryness, L²H₄ (59 mg, 59%) was isolated as a beige solid as its tetrahydrochloride salt. ¹H NMR (CD₃OD, 200 MHz): $\delta = 3.6$ –3.9 (brm, 4H), 4.34 (s, 4H), 4.73 (s, 4H), 8.20 (d, ³ $J = 7.6$ Hz, 2H), 8.29–8.43 (m, 4H), 8.72–8.80 (m, 4H), 8.89 ppm (d, ³ $J = 7.6$ Hz, 2H); ¹³C NMR (CD₃OD, 50 MHz): $\delta = 51.6$, 55.2, 56.4, 57.7, 125.2, 126.2, 127.5, 129.1, 129.3, 142.4, 148.3, 148.6, 149.0, 155.1, 166.6, 168.7 ppm; MS (FAB⁺): m/z (%): 601.2 (20) [L²H₄+H]⁺; elemental analysis calcd (%) for C₃₀H₂₈N₆O₈·4HCl·2H₂O: C 46.04, H 4.65, N 10.74; found: C 45.88, H 4.51, N 10.49.

Preparation of ligand $L^3H_3\cdot 3HCl$: Compound **14** (142 mg, 0.24 mmol) was dissolved in MeOH (20 mL) and water (20 mL) containing NaOH (33 mg, 0.83 mmol) was added. The solution was heated at 60 °C for 5 h, cooled, concentrated to approximately 10 mL under reduced pressure, and washed with CH_2Cl_2 (20 mL). The pH of the aqueous layer was adjusted to 1 with concd HCl and the solvent was evaporated. The solid was triturated with MeOH (3 mL), the insoluble white solid was filtered and addition of THF resulted in the formation of a yellowish precipitate which was isolated by centrifugation and dried under reduced pressure to yield $L^3H_3\cdot 3HCl$ (126 mg, 82%) as a pale yellow solid. 1H NMR (CD_3OD , 200 MHz): δ = 4.18–4.42 (m, 3H), 4.92 (s, 4H), 8.02–8.12 (m, 4H), 8.22 (d, 3J = 7.8 Hz, 2H), 8.46 (t, 3J = 7.6 Hz, 2H), 8.56 (d, 3J = 7.8 Hz, 2H), 8.66 ppm (d, 3J = 8.0 Hz, 2H); IR (KBr): $\tilde{\nu}$ = 2974 (w), 2901 (w), 1719 (s), 1629 (s), 1262 (m), 1049 cm^{-1} (m); UV/Vis (0.01 M Tris/HCl buffer, pH 7.0): λ_{max} (ϵ_{max}) = 239 (20300), 288 nm (24800); MS (FAB⁺): m/z (%): 530.2 (20) [$L^3H_3 + H$]⁺; elemental analysis calcd (%) for $C_{27}H_{23}N_5O_7\cdot 3HCl$: C 50.75, H 4.11, N 10.96; found: C 50.63, H 4.38, N 10.82.

Preparation of ligand $L^4H_3\cdot 3HCl\cdot 3H_2O$: A solution of compound **17** (103 mg, 0.16 mmol) and NaOH (50 mg, 1.25 mmol) in a mixture of methanol (10 mL) and water (5 mL) was heated to 70 °C for 5 h. The solution was evaporated to dryness and the resulting solid was dissolved in water (8 mL). At 0 °C, aqueous HCl (1 N) was slowly added until a precipitate appeared (pH 4–5). Upon centrifugation, $L^4H_3\cdot 3HCl\cdot 3H_2O$ (59 mg, 53%) was isolated as a white powder. 1H NMR (NaOD/*t*BuOH, 300 MHz): δ = 3.75 (s, 4H), 4.04 (s, 1H), 6.84 (d, 3J = 7.5 Hz, 2H), 7.15–7.26 (m, 4H), 7.32 (d, 3J = 7.5 Hz, 2H), 7.42 (t, 3J = 7.5 Hz, 2H), 7.56 ppm (d, 3J = 7.5 Hz, 2H); ^{13}C NMR (NaOD/*t*BuOH, 75 MHz): δ = 60.3, 79.4, 119.9, 122.9, 124.1, 124.4, 138.2, 138.6, 152.8, 153.7, 154.0, 158.7, 172.3, 177.3 PPM; IR (KBr): $\tilde{\nu}$ = 3443 (s), 2913 (w), 2846 (w), 1720 (m, C=O), 1622 (m, COO_{asym}), 1448 (w), 1384 (m), 1356 (m, COO_{sym}), 1249 (w), 1169 cm^{-1} (w); UV/Vis (0.01 M Tris/HCl buffer, pH 7.0): λ_{max} (ϵ_{max}) = 239 (20300), 288 nm (24800); MS (FAB⁺): m/z (%): 544.2 (20) [$L^4H_3 + H$]⁺; elemental analysis calcd (%) for $C_{27}H_{21}N_5O_8\cdot 3HCl\cdot 3H_2O$: C 45.87, H 4.28, N 9.91; found: C 45.75, H 4.09, N 9.78.

Preparation of ligand $L^5Na_4\cdot 5H_2O$: Compound **20** (51 mg, 65 μ mol) was dissolved in aqueous NaOH (6 mL, 0.05 N). The solution was heated to 100 °C for 19 h. After cooling to RT, the aqueous layer was extracted four times with CH_2Cl_2 (5 mL) and evaporated to dryness. Upon precipitation in a H_2O /THF mixture, $L^5Na_4\cdot 5H_2O$ (45 mg, 79%) was isolated as a beige powder. 1H NMR (300 MHz, D_2O /*t*BuOH): δ = 1.18 (t, 3J = 7.0 Hz, 6H), 2.06–2.27 (m, 2H), 2.37–2.58 (m, 2H), 3.50 (t, 3J = 7.5 Hz, 1H), 3.86–3.99 (m, 4H), 4.02–4.24 (m, 4H), 7.48 (d, 3J = 7.0 Hz, 2H), 7.59–7.81 ppm (m, 10H); ^{13}C NMR (75 MHz, D_2O /*t*BuOH): δ = 16.4, 16.5, 27.8, 35.6, 59.8, 62.4, 62.5, 71.6, 121.2, 124.0, 124.1, 125.7, 127.1, 127.4, 138.0, 138.2, 138.5, 154.6, 155.0, 156.3, 156.6, 157.8, 160.6, 181.1, 183.6 ppm; ^{31}P NMR (162 MHz, D_2O): δ = 10.17 ppm; IR (KBr): $\tilde{\nu}$ = 3450 (s), 1637 (m, COO_{asym}), 1384 (m, COO_{sym}), 1215 (w, P=O), 1149 (w), 1063 (w), 1030 cm^{-1} (w); MS (FAB⁺): m/z (%): 764.2 (10) [$Na_4L^5 - Na$]⁺; elemental analysis calcd (%) for $C_{31}H_{31}N_5Na_4O_{10}P_2\cdot 5H_2O$: C 42.43, H 4.71, N 7.98; found: C 42.35, H 4.55, N 7.78.

Preparation of compound $L^6Na_6\cdot 2H_2O\cdot NaBr$: Compound **20** (65 mg, 83 μ mol) and trimethylsilyl bromide (165 μ L, 1.2 mmol) were dissolved in CH_2Cl_2 (10 mL). The solution was stirred at RT under argon for 17 h, and was evaporated to dryness. Trimethylsilyl bromide (165 μ L, 1.2 mmol) and $CHCl_3$ (10 mL) were added and the resulting solution was refluxed for 3 h. After evaporation of the solvent, NaOH (20 mg, 0.5 mmol) and water (5 mL) were added and the solution was heated to 80 °C for 31 h. The solution was evaporated to dryness, the residue was solubilised in a mixture of methanol and water, and the product was precipitated by addition of THF. Upon centrifugation, $L^6Na_6\cdot 2H_2O\cdot NaBr$ (54 mg, 71%) was isolated as a yellow powder. 1H NMR (300 MHz, D_2O /*t*BuOH): δ = 2.06–2.18 (m, 2H), 2.36–2.48 (m, 2H), 3.45 (t, 3J = 7.0 Hz, 1H), 4.03–4.21 (m, 4H), 7.51 (d, 3J = 7.5 Hz, 2H), 7.67–7.87 ppm (m, 10H); ^{13}C NMR (75 MHz, D_2O /*t*BuOH): δ = 27.5, 35.6, 59.1, 70.5, 121.5, 122.5, 124.9, 126.1, 126.4, 137.6, 137.7, 138.7, 155.4, 155.7, 155.8, 160.4, 163.4, 164.7, 181.2, 183.6 ppm; ^{31}P NMR (162 MHz, D_2O): δ = 7.90 ppm; IR (KBr): $\tilde{\nu}$ = 3451 (s), 1637 (m, COO_{asym}), 1384 (m, COO_{sym}), 1076 cm^{-1}

(w); UV/Vis (0.01 M Tris/HCl buffer, pH 7.0): λ_{max} (ϵ_{max}) = 237 (11400), 289 nm (14700); elemental analysis calcd (%) for $C_{27}H_{21}N_5Na_6O_{10}P_2\cdot 2H_2O\cdot NaBr$: C 35.47, H 2.76, N 7.66; found: C 35.75, H 3.03, N 7.62.

Preparation of compound $[Eu(L^1)]\cdot 6H_2O$: Ligand $L^1H_3\cdot 4HCl$ (22 mg, 30 μ mol) was dissolved in a mixture of methanol (10 mL) and water (10 mL), and $EuCl_3\cdot 6H_2O$ (12 mg, 33 μ mol) in methanol (3 mL) and water (3 mL) was added. The solution was heated to 70 °C for 1 h. After cooling to RT, the pH was adjusted to 7.0 with a 0.5% NaOH solution in water, and the solution was evaporated to dryness. The residue was dissolved in methanol and filtered over Celite, and the product was precipitated with Et_2O . Upon centrifugation, $[Eu(L^1)]\cdot 6H_2O$ (24 mg, 95%) was isolated as a white powder. IR (KBr): $\tilde{\nu}$ = 3436 (s), 1636 (m, COO_{asym}), 1432 (w), 1384 (m, COO_{sym}), 1258 (w), 1086 (w), 1016 cm^{-1} (w); UV/Vis (0.01 M Tris/HCl buffer, pH 7.0): λ_{max} (ϵ_{max}) = 273 (9500), 297 (9200), 321 nm (5100); MS (FAB⁺): m/z (%): 725.2 (85) $[Eu(L^1) + H]^+$, 727.1 (100) $[Eu(L^1) + H]^+$; elemental analysis calcd (%) for $C_{31}H_{21}EuN_6O_6\cdot 6H_2O$: C 44.67, H 3.99, N 10.08; found: C 44.59, H 3.56, N 9.91.

Preparation of compound $[Tb(L^1)]\cdot 5H_2O$: Ligand $L^1H_3\cdot 4HCl$ (20 mg, 28 μ mol) was dissolved in a mixture of methanol (10 mL) and water (10 mL), and $TbCl_3\cdot 6H_2O$ (11 mg, 30 μ mol) in methanol (3 mL) and water (3 mL) was added. The solution was heated to 70 °C for 1 h. After cooling to RT, the pH was adjusted to 7.1 with a 0.5% NaOH solution in water, and the solution was evaporated to dryness. The residue was dissolved in methanol and filtered over Celite, and the product was precipitated with Et_2O . Upon centrifugation, $[Tb(L^1)]\cdot 5H_2O$ (19 mg, 84%) was isolated as a white powder. IR (KBr): $\tilde{\nu}$ = 3434 (s), 1636 (m, COO_{asym}), 1587 (m, COO_{asym}), 1474 (w), 1384 (m, COO_{sym}), 1262 (w), 1169 (w), 1083 (w), 1023 cm^{-1} (w); UV/Vis (0.01 M Tris/HCl buffer, pH 7.0): λ_{max} (ϵ_{max}) = 272 (8500), 297 (9000), 318 nm (5200); MS (FAB⁺): m/z (%): 733.4 (80) $[Tb(L^1) + H]^+$; elemental analysis calcd (%) for $C_{31}H_{21}N_6O_6Tb\cdot 5H_2O$: C 45.27, H 3.80, N 10.22; found: C 44.97, H 3.25, N 10.02.

Preparation of compound $(Et_3NH)[Eu(L^2)]\cdot 4H_2O$: In a solution of MeOH (20 mL) and water (5 mL) were dissolved ligand $L^2H_4\cdot 4HCl\cdot 2H_2O$ (25 mg, 35 μ mol) and $EuCl_3\cdot 6H_2O$ (14 mg, 38 μ mol). The solution was heated to 60 °C for 3 h, cooled to RT, and concentrated to 5 mL. Et_3N was added to bring the pH to 8–9 and the solution was evaporated to dryness. The residue was dissolved in H_2O (10 mL), and the aqueous phase was washed twice with CH_2Cl_2 (15 mL), and evaporated to dryness. The solid was dissolved in a minimum amount of MeOH and addition of Et_2O resulted in the formation of a white precipitate, which was collected by centrifugation and dried under vacuum to afford $(Et_3NH)[Eu(L^2)]\cdot 4H_2O$ (17.7 mg, 51%). IR (KBr): $\tilde{\nu}$ = 3420 (s), 1592 (s, COO_{asym}), 1460 (m), 1420 (m), 1384 (m, COO_{sym}), 1254 (w), 1090 (w), 1013 (w), 776 cm^{-1} (w); MS (FAB⁻): m/z (%): 749.3 (100) $[Eu(L^2)]^-$; elemental analysis calcd (%) for $C_{36}H_{40}EuN_7O_8\cdot 4H_2O$: C 46.85, H 5.25, N 10.63; found: C 46.78, H 5.17, N 10.42.

Preparation of compound $(Et_3NH)[Tb(L^2)]\cdot 3H_2O$: The compound was obtained similarly to the europium one starting from $L^2H_4\cdot 4HCl\cdot 2H_2O$ (20 mg, 28 μ mol) and $TbCl_3\cdot 6H_2O$ (10.5 mg, 28 μ mol) to give $(Et_3NH)[Tb(L^2)]\cdot 4H_2O$ (21.3 mg, 78%). Elemental analysis calcd (%) for $C_{36}H_{40}TbN_7O_8\cdot 3H_2O$: C 47.42, H 5.09, N 10.75; found: C 47.32, H 4.89, N 10.58.

Preparation of compound $[Eu(L^3H_2Cl)]Cl\cdot 3H_2O$: Ligand $L^3H_3\cdot 3HCl$ (41.6 mg, 65 μ mol) and $EuCl_3\cdot 6H_2O$ (24 mg, 65 μ mol) were dissolved in MeOH (25 mL) and the solution was refluxed for 3 h. The solvent was removed under reduced pressure, the residue was redissolved in MeOH (3 mL) and THF (12 mL) was added, resulting in the formation of a voluminous white precipitate. The solution was filtered over Celite and was allowed to concentrate by slow evaporation of the solvent. White crystals formed and were recovered by removal of the solvent. The crystals were dried under reduced pressure to afford $[Eu(L^3H_2Cl)]Cl\cdot 3H_2O$ (24 mg, 51%). IR (KBr): $\tilde{\nu}$ = 3347 (s, br), 3070 (w), 1737 (w, COOH_{asym}), 1625, 1593 (m, COO_{asym}), 1572 (w), 1439 (w), 1415 (w), 1378 (m, COO_{sym}), 1273 (w), 1252 (w), 1187 (w), 1012 (w), 773 cm^{-1} (m); MS (FAB⁺): m/z (%): 714.2 (100) $[Eu(L^3H_2Cl)]^+$, 339.6 (20) $[Eu(L^3H_2)]^{2+}$; elemental analysis

calcd (%) for $C_{27}H_{28}EuN_5O_4Cl_2$: C 39.47, H 3.44, N 8.53; found: C 39.19, H 3.42, N 8.37.

Preparation of compound [Eu(L³)(H₂O)]·NaCl: Ligand L³H₃·3HCl (41.6 mg, 65 μmol) and EuCl₃·6H₂O (24 mg, 65 μmol) were dissolved in 25 mL MeOH and the solution was heated to reflux for 3 h. The solvent was removed under reduced pressure, the residue redissolved in water (10 mL), and the pH was slowly raised by addition of diluted NaOH in water. Around pH 4–5, a voluminous precipitate formed which was collected by centrifugation, was washed successively with MeOH and THF, and was dried under reduced pressure to afford [Eu(L³)(H₂O)]·NaCl (33 mg, 67%) as a white solid. IR (KBr): $\tilde{\nu}$ = 3407 (s), 3264 (s), 3096 (w), 1606 (s, COO_{asym}), 1583 (s, COO_{asym}), 1461 (w), 1411 (m), 1371 (m, COO_{sym}), 1273 (w), 1010 (w), 784 cm⁻¹ (w); MS (FAB⁺): *m/z* (%): 680.2 (100) [Eu(L³+H)]⁺, 648.1 (30) [Eu(L³-CH₂OH)]⁺; elemental analysis calcd (%) for $C_{27}H_{20}N_5O_7Eu\cdot NaCl$: C 42.95, H 2.94, N 9.28; found: C 42.56, H 2.61, N 8.90.

Acknowledgements

The French Ministère de la Recherche et de l'Enseignement Supérieur is gratefully acknowledged for financial support (N.W.).

- [1] a) E. Toth, L. Helm, A. E. Merbach in *The Chemistry of Contrast Agents in Medical Magnetic Resonance Imaging* (Eds.: A. E. Merbach, E. Toth), Wiley, Chichester, **2001**, pp. 45–119; b) R. B. Laufer, *Chem. Rev.* **1987**, *87*, 901; c) P. Caravan, J. J. Ellison, T. J. McMurry, R. B. Laufer, *Chem. Rev.* **1999**, *99*, 2293.
- [2] a) J. Wöhnert, K. J. Franz, M. Nitz, B. Imperiali, H. Schwalbe, *J. Am. Chem. Soc.* **2003**, *125*, 13338; b) M. Prudêncio, J. Rohovec, J. A. Peters, E. Tocheva, M. J. Boulanger, M. E. P. Murphy, H. J. Hupkes, W. Kosters, A. Impagliazzo, M. Ubbink, *Chem. Eur. J.* **2004**, *10*, 3252; c) C. Reilley, B. W. Good, *Anal. Chem.* **1975**, *47*, 2110.
- [3] R. S. Prosser, H. Bryant, R. G. Bryant, R. R. Vold, *J. Magn. Reson.* **1999**, *141*, 256.
- [4] a) I. Hemmila, V.-M. Mukkala, *Crit. Rev. Clin. Lab. Sci.* **2001**, *38*, 441; b) I. Hemmila, S. Webb, *Drug Discovery Today* **1997**, *2*, 373; c) P. R. Selvin, *Annu. Rev. Biophys. Biomol. Struct.* **2002**, *31*, 275.
- [5] a) J.-C. G. Bünzli, C. Piguet, *Chem. Soc. Rev.* **2005**, *34*, 1048; b) J.-C. G. Bünzli, *Acc. Chem. Res.* **2006**, *39*, 53.
- [6] a) N. Sabbatini, M. Guardigli, J.-M. Lehn, *Coord. Chem. Rev.* **1993**, *123*, 201; b) S. I. Weissmann, *J. Chem. Phys.* **1942**, *10*, 214.
- [7] a) W. D. W. Horrocks, Jr., D. R. Sudnick, *J. Am. Chem. Soc.* **1979**, *101*, 334; b) A. Beeby, I. M. Clarkson, R. S. Dickins, S. Faulkner, D. Parker, L. Royle, A. S. de Sousa, J. A. G. Williams, M. Woods, *J. Chem. Soc. Perkin Trans. 2* **1999**, 493; c) R. M. Supkowski, W. D. W. Horrocks, Jr., *Inorg. Chim. Acta* **2002**, *340*, 44.
- [8] G. A. Hebbink, D. N. Reinhoudt, F. C. J. M. van Veggel, *Eur. J. Inorg. Chem.* **2001**, 4101.
- [9] a) M. Latva, H. Takalo, V.-M. Mukkala, C. Matachescu, J. C. Rodriguez-Ubis, J. Kankare, *J. Lumin.* **1997**, *75*, 149; b) F. J. Steemers, W. Verboom, D. N. Reinhoudt, E. B. van der Tol, J. W. Verhoeven, *J. Am. Chem. Soc.* **1995**, *117*, 9408; c) S. Quici, G. Marzanni, M. Cavazzini, P. L. Anelli, M. Botta, E. Giuanolio, G. Accorsi, G. Armaroli, N. Armaroli, F. Barigelletti, *Inorg. Chem.* **2002**, *41*, 2777; d) S. W. Magennis, S. Parsons, Z. Pikramenou, *Chem. Eur. J.* **2002**, *8*, 5761.
- [10] C. Yang, L.-M. Fu, Y. Wang, J.-P. Zhang, W.-T. Wong, X.-C. Ai, Y.-F. Qiao, B.-S. Zou, L.-L. Gui, *Angew. Chem.* **2004**, *116*, 5120; *Angew. Chem. Int. Ed.* **2004**, *43*, 5010.
- [11] N. Weibel, L. Charbonnière, M. Guardigli, A. Roda, R. Ziessel, *J. Am. Chem. Soc.* **2004**, *126*, 4888.
- [12] L. Charbonnière, N. Weibel, C. Estournes, C. Leuvrey, R. Ziessel, *New J. Chem.* **2004**, *28*, 777.
- [13] N. Hildebrandt, L. Charbonnière, H.-G. Löhmansröben, R. Ziessel, *Angew. Chem.* **2005**, *117*, 7784; *Angew. Chem. Int. Ed.* **2005**, *44*, 7612.
- [14] S. Aime, E. Gianolo, D. Corpillo, C. Cavallotti, G. Palmisano, M. Sisti, G. B. Giovenzana, R. Pagliarin, *Helv. Chim. Acta* **2003**, *86*, 615.
- [15] a) S. Aime, M. Botta, S. Geninatti Crich, G. Giovenzana, R. Pagliarin, M. Sisti, E. Terreno, *Magn. Reson. Chem.* **1998**, *36*, S200; b) M. Botta, *Eur. J. Inorg. Chem.* **2000**, 399.
- [16] S. Mameri, L. J. Charbonnière, R. Ziessel, *Synthesis* **2003**, *17*, 2713.
- [17] A. El Ghayoury, R. Ziessel, *J. Org. Chem.* **2000**, *65*, 7757.
- [18] a) V. Penicaud, F. Odobel, B. Bujoli, *Tetrahedron Lett.* **1998**, *39*, 3869; b) S. Comby, D. Imbert, A.-S. Chauvin, J.-C. G. Bünzli, L. J. Charbonnière, R. F. Ziessel, *Inorg. Chem.* **2004**, *43*, 7369.
- [19] T. H. Fife, T. J. Przystas, *J. Am. Chem. Soc.* **1982**, *104*, 2251.
- [20] A similar protocol was described for methoxy esters: S. Jew, B. Park, D. Lim, M. G. Kim, I. K. Chung, C. I. Hong, J.-K. Kim, H.-J. Park, J.-H. Lee, H. Park, *Bioorg. Med. Chem. Lett.* **2003**, *13*, 609.
- [21] R. Fornassier, D. Milani, P. Scrimin, U. Tonellato, *J. Chem. Soc. Perkin Trans. 2* **1986**, 233.
- [22] K. B. Jensen, T. M. Braxmeier, M. Demarcus, J. G. Frey, J. D. Kilburn, *Chem. Eur. J.* **2002**, *8*, 1300.
- [23] M. Montalti, S. Wadhwa, W. Y. Kim, R. A. Kipp, R. H. Schmehl, *Inorg. Chem.* **2000**, *39*, 76.
- [24] a) P. Krumholz, *J. Am. Chem. Soc.* **1951**, *73*, 3487; b) K. Nakamoto, *J. Phys. Chem.* **1960**, *64*, 1420.
- [25] a) L. J. Charbonnière, R. Ziessel, M. Montalti, L. Prodi, N. Zaccheroni, C. Boehme, G. Wipff, *J. Am. Chem. Soc.* **2002**, *124*, 7779; b) M. Montalti, L. Prodi, N. Zaccheroni, L. Charbonnière, L. Douce, R. Ziessel, *J. Am. Chem. Soc.* **2001**, *123*, 12694.
- [26] a) N. Chatterton, Y. Bretonnière, J. Pécaut, M. Mazzanti, *Angew. Chem.* **2005**, *117*, 7767; *Angew. Chem. Int. Ed.* **2005**, *44*, 7595; b) N. Weibel, L. Charbonnière, R. Ziessel, *Tetrahedron Lett.* **2006**, *47*, 1793.
- [27] a) S. Mameri, L. J. Charbonnière, R. Ziessel, *Inorg. Chem.* **2004**, *43*, 1819; b) L. J. Charbonnière, R. Schurhammer, S. Mameri, G. Wipff, R. F. Ziessel, *Inorg. Chem.* **2005**, *44*, 7151.
- [28] Y. Bretonnière, M. Mazzanti, J. Pécaut, F. A. Dunand, A. E. Merbach, *Chem. Commun.* **2001**, 621.
- [29] F. Renaud, C. Piguet, G. Bernardinelli, J.-C. G. Bünzli, G. Hopfgartner, *J. Am. Chem. Soc.* **1999**, *121*, 9326.
- [30] S. Comby, R. Scopelliti, D. Imbert, L. Charbonnière, R. Ziessel, J.-C. G. Bünzli, *Inorg. Chem.* **2006**, *45*, 3158.
- [31] C. Piguet, G. Bernardinelli, G. Hopfgartner, *Chem. Rev.* **1997**, *97*, 2005.
- [32] R. Ziessel, L. J. Charbonnière, M. Cesario, T. Prangé, M. Guardigli, A. Roda, A. Van Dorselaer, H. Nierengarten, *J. Supramol. Chem.* **2003**, *15*, 277.
- [33] L. J. Charbonnière, R. Ziessel, M. Guardigli, A. Roda, N. Sabbatini, M. Cesario, *J. Am. Chem. Soc.* **2001**, *123*, 2436.
- [34] J. Bernstein, R. E. Davis, L. Shimon, N. E. Chang, *Angew. Chem.* **1995**, *107*, 1689; *Angew. Chem. Int. Ed. Engl.* **1995**, *34*, 1555.
- [35] H. Gottlieb, V. Kotlyar, A. Nudelman, *J. Org. Chem.* **1997**, *62*, 1997.
- [36] Y. Haas, G. Stein, *J. Phys. Chem.* **1971**, *75*, 3668.
- [37] K. Nakamura, *Bull. Chem. Soc. Jpn.* **1982**, *55*, 2697.
- [38] J. Olmsted, *J. Phys. Chem.* **1979**, *83*, 2581.
- [39] B. Valeur in *Molecular Fluorescence*, Wiley-VCH, Weinheim, **2002**, p. 161.
- [40] B. V. Nonius, "Collect" Data Collection Software, **1999**.
- [41] "Macromolecular Crystallography, Part A": Z. Otwinowski, W. Minor, *Methods Enzymol.* **1997**, 307.
- [42] G. M. Sheldrick, SHELX97, Program for the Refinement of Crystal Structures from Diffraction Data, University of Göttingen, Göttingen (Germany), **1997**.

Received: June 27, 2006
Published online: September 29, 2006